ON THE FOUNDATION OF CIRCULAR-SAW STABILITY THEORY[1]

C. D. Mote, Jr. and *L. T. Nieh*[2, 3]

ABSTRACT

The buckling and critical speed saw stability theories for predicting the flatness of a circular saw are discussed. Laboratory experiments were performed for evaluation of the stability concepts. The experiments include accurate measurement of the saw-disc natural frequencies or frequency spectrum and the measurement and inclusion of thermal effects in saw-disc stability analysis.

Additional keywords: Stability, critical speed, buckling, cutting accuracy, rotating disc, thermal stress, temperature, radiation, vibration, numerical analysis, natural frequencies, spectrum.

INTRODUCTION

There are many approaches to the problem of designing thin saw blades to cut straight. The fastest, often the easiest, and sometimes the only available method in optimal design relies upon genius of insight and invention. Here, the engineer tries a new saw design or production process specification to see what happens. The principal advantage of this technique is its speed. He quickly learns if some procedure does or does not work, and application of results is immediate because his attention is focused on the specific problem of his interest. However, the depth of understanding of the physical process accompanying this design procedure is necessarily shallow. From the try-and-see approach one gains little general perspective on the problem from which he can explain broader observations, predict what would happen with proposed design changes, etc. On the other hand if one is able to develop a somewhat general theoretical model of a physical system such as a circular saw, which includes "all" significant effects governing its behavior, then one can relate the design parameters to the system performance.

The general-view approach does not eliminate try-and-see studies, but it guides one's thinking to designs that are more likely to be satisfactory and away from many fundamentally poor ones. In circular saws, for example, there are an infinite number of possible designs if one considers variations in thickness, clamping radius, rotation speed, slots, holes, etc. Variation in saw material properties alone makes design evaluation difficult. Also each saw design must be evaluated in the appropriate operational environment; a saw that is optimal in the intended environment of operation may be unsatisfactory in the environment of evaluation. Accordingly, specification of the optimal design implies a clear understanding of the operational environment. It is probably impossible to optimally design a saw and the process environment by trial-and-error techniques.

The present and probably continuing trend in industry is toward more efficient and more precise machining, requiring nearly optimal saw design and optimal process control. It is the opinion of the writers that the optimal saw design and operation question must be approached from the basis of a sound stability theory

[1] This paper was presented at Session 13—Milling and Machining—of the 26th Annual Meeting of the Forest Products Research Society, 20 June 1972 in Dallas, TX.

[2] The authors are, respectively, Professor, Mechanical Engineering and Research Engineer, Forest Products Laboratory, University of California, Berkeley; and Research Assistant, University of California Forest Products Laboratory, Richmond, CA; presently Research Engineer, General Electric Co., Louisville, KY.

[3] The authors gratefully acknowledge partial support of their project by McIntire-Stennis funds, by California Cedar Products Co., and by California Saw, Knife and Grinding Works, Inc.

that incorporates all major influences on the saw vibrational response. The present research on the foundations of the stability theory, outlined in this paper, was guided by this viewpoint. The focus of our most recent research efforts has been to test the theoretical stability analysis and to measure the temperature distribution.

This paper is directed toward both the theoretical concept of instability in circular saws and the experiments focused on evaluation of these concepts. The experiments include accurate measurement of the disc natural frequencies or frequency spectrum, and the measurement and inclusion of thermal effects on disc stability.

TYPES OF INSTABILITY

When a saw no longer is flat, conditions unacceptable for operation result. Herein, an unstable saw is defined to be one whose equilibrium geometry is no longer flat (within a tolerance), and an unstable environment is defined to be any set of design and operating conditions that results in a nonflat saw. The condition of impending instability is of principal concern, as this marks the transition from a stable (flat) to an unstable (nonflat) saw. All stability research to date has in effect been focused on identification of impending instability conditions.

Two characteristic types of instability have been observed in saws, and others are possible but have not been identified. The first is termed "buckling instability." Here the saw's peripheral edge assumes a wavy or harmonic shape with amplitudes of one or more saw-thicknesses. For instance, in a saw having one complete wave around the periphery, there is one saw-diameter that is coincident with the diameter in the original stable (or flat) saw. This would be termed a 1-nodal-diameter buckling mode. Typically, a 16-inch-diameter saw can be expected to buckle in a mode of either 2-, 3-, 4-, 5-, or 6-nodal diameters, with 3, 4, or 5 being the most commonly observed in our work. Specific design and operating conditions explicitly define the particular mode. If a saw buckles in the 4-nodal diameter mode, then the edge assumes four complete waves that are *fixed* on the saw disc. As the buckled saw passes through the workpiece, the waves in the saw edge cut an oscillating path, which is recognized as a rather high frequency "snaking saw." Typically, the saw interacts with the workpiece, the saw temperature increases, which enhances or maintains the instability, and workpiece dimensional accuracy is lost. The amplitude of the buckled saw displacement may be small (say ½–1 plate thickness) depending upon postbuckling effects such as workpiece-saw interaction. In many respects small amplitude buckling is a more serious problem, as it is more difficult to observe but still renders the product unacceptable. One can think of buckling as a "terminal" instability, which is a rather advanced form of instability and probably not the one that occurs first.

The second type of instability is termed "critical speed instability." Here, the motion of the cutting force around the saw's periphery excites the saw into a standing-wave resonance. In this case the wave or nodal diameter mode is fixed in space (not on the saw) and the saw rotates through it. In effect, the saw loses stiffness in one of its lateral modes and any lateral force thus causes relatively large lateral saw displacements, which results in instability. Often, just prior to the formation of the standing wave, a backward traveling wave can be observed that gives the saw edge a relatively low frequency oscillation. This signals the approach of the standing wave instability and gives rise to the low frequency "snaking" commonly observed. The critical speed instability condition is reached before the buckling instability condition. In other words, conditions inducing critical speed instability are the same as those causing buckling. However, the critical speed instability always appears to be induced before buckling, so recent studies have therefore focused upon identifying critical speeds (Nieh and Mote 1972; Mote 1970a, 1971, 1972; Mote and Nieh 1971; Dugdale 1966). Both types of instability are controlled by saw geometry, clamping

or edge conditions, rotation speed, tension or intitial stresses, and thermal effects. Numerical techniques have been recently developed for prediction of both impending instability conditions when the aforementioned effects are included (Nieh and Mote 1972; Mote 1970a, 1972; Mote and Nieh 1971).

In measuring critical speed conditions, there are two quantities of principal interest: (1) the rotation speed at which the standing wave forms, and (2) the mode or number of waves (nodal diameters) associated with the standing wave shape. In order to measure both quantities a carbon brush-light panel system was developed (Dugdale 1966; Mote 1971; Mote and Nieh 1971). At instability the deformed disc contacts the brushes, closes the individual simple circuits, and a light corresponding to each brush contact is illuminated. The mode is identified in the stationary light panel array, and simultaneously the rotation speed is measured with a digital counter.

It appears unlikely that any saw can operate effectively above its critical speed. Variation in the environment alters the critical speed, and in fact the critical speed varies continuously during a production process. The primary source of variability results from thermal effects, which have an influence probably far greater than is generally imagined. When the critical speed is reduced to the operating speed of the saw, instability occurs immediately. As long as the critical speed remains above the operating speed, stable saw operation is possible. Once instability occurs there is little chance for self-correction. For process control, instability must be predicted and prevented prior to its occurrence rather than by trying to impose postinstability corrections.

Tensioning can be viewed as a process that favorably alters conditions under which a critical speed or buckling instability occurs. Any phenomenon that induces stresses in the saw alters the critical speed. The normal tensioning procedure shifts the critical speed upward (Mote and Nieh 1971). Upward shifts in critical speed are desirable for two reasons. First, they increase the separation between the operating and critical speed, which reduces the likelihood of instability due to process-induced critical speed variations. Second, they allow saw design modifications that have a tendency to reduce the critical speed but are economically more desirable—e.g., reducing saw thickness and kerf.

The skilled saw-fiber often tests "proper" tension by placing a straight edge across the saw blade diameter to measure the saw's dishing or buckling. Here, one may ask what that has to do with the critical speed. The connection is indirect but clear. The saw buckling measured by the filer is the result of the initial or tension stress state. The filer obtains a qualitative measure of the initial stress state which, in turn, shifts the critical speed. It is understandable that the technique of tensioning can shift the critical speed either up or down, depending upon the initial stress state resulting from the procedure.

STABILITY ANALYSIS

Stability theories used to predict impending instability utilize disc natural frequencies or disc-frequency spectrum as their basis. (For a detailed discussion of these theories see Dugdale 1966; Mote 1970a, 1971, 1972; Mote and Nieh 1971; Nieh and Mote 1972.) In brief, buckling instability occurs when one disc natural frequency is driven to zero by a change in the disc effective stiffness; $\omega_n \to 0$. A critical speed occurs when the backward traveling wave component of one of the natural frequencies becomes stationary in space; $\omega_n - n\omega \to 0$ where $\omega_n =$ nth natural frequency, n is number of nodal diameters of that mode, and ω is the rotation speed. Shifts in critical speed or buckling conditions are caused by variations in the frequency spectrum. Measurement or computation of the spectrum permits accurate estimation of the degree of stability or the proximity of instability. Figure 1 data give spectral shifts from peripheral heating

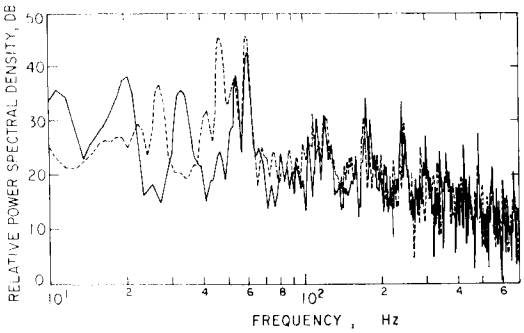

FIG. 1. Frequency response spectrum of a uniform disc solid—without thermal excitation Dash—with peripheral heating $\omega = 60$ rev/sec, $b = 8.0$ inches, $a = 4.0$ inches, $t = 0.040$ inch.

of the disc; note in Figs. 1 and 2 the increased complexity of the spectrum caused by rotation, as viewed by the stationary observer. The peaks of these curves indicate the resonant frequencies as seen by the stationary observer. These frequencies can be compared with theoretical computations based upon the finite element model of Fig. 3 (Mote 1970a, 1972). Models of this type are particularly suitable for the complex geometries of saws because the element configuration is highly flexible. It should be noted that the technique has important application to the saw thermal analysis, as well as to membrane stress and vibration problems. The experimental resonant frequencies, as in Fig. 1, the theoretical resonant frequencies from a model such

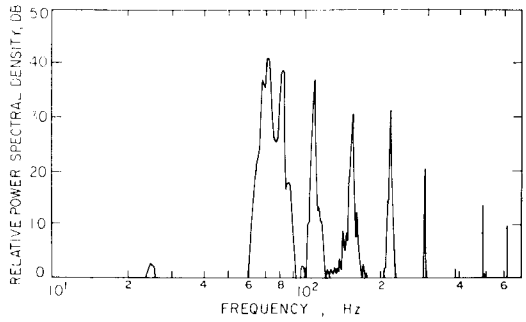

FIG. 2. Frequency response spectrum of a stationary uniform disc without thermal excitation $\omega = 0$ rev/sec $b = 8.0$ inches, $a = 4.0$ inches, $t = 0.040$ inch.

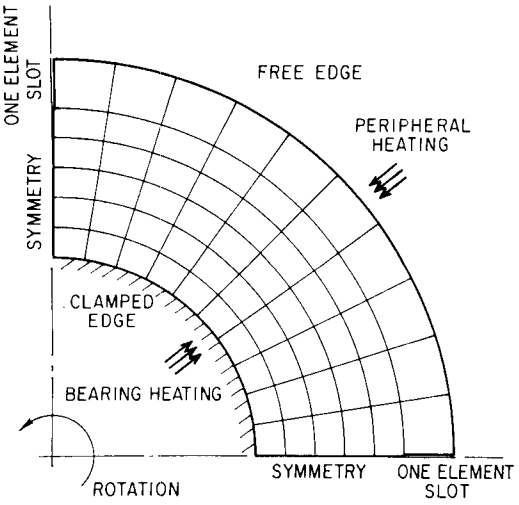

FIG. 3. Finite element mesh for stress and spectral analysis.

as shown in Fig. 3, and the critical speed experiments from the light panel system are compared for one example in Fig. 4. For a rotation speed greater than zero the stationary observer sees two resonant frequencies for each node n greater than zero. The higher frequency corresponds to the resonance of the forward traveling wave (the wave propagating in the direction of disc rotation), and the lower frequency corresponds to the backward traveling wave resonance. Note that there is only one resonance for a stationary disc or for an observer rotating with the disc. Relative to the disc, the forward and backward waves travel in opposite directions at the same speed; their speed relative to the ground or stationary observer is shifted by the disc rotation. The comparison of theoretical curves and experimental points is excellent; in particular, the critical speed of the uniform disc predicted by theory and confirmed by the data points is 59.2 rev/sec in the 4-nodal diameter mode. The light panel test determined the critical speed to be 60.8 rev/sec.

The numerical flexibility of the theoretical methods employed is demonstrated in Fig. 4, where four 1-inch slots are numerically cut into the disc periphery (Fig. 3).

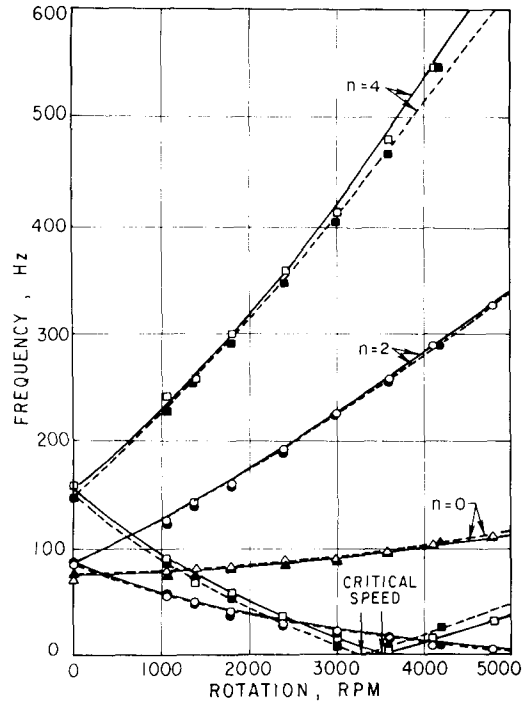

FIG. 4. Resonant frequencies of a disc without thermal excitation. Curves are theoretical and points are spectral analysis data. Solid curve for uniform disc. Dash curve for disc with 4–1″ slots. n = no. of nodal da., b = 8.0 inches, a = 4.0 inches, t = 0.040 inch.

The result shows that cutting such slots into a cold disc reduces the critical speed 8% from 59.2 rev/sec to 55.3 rev/sec. If the slots are extended to 2 inches, the critical speed is reduced 20% to 44.7 rev/sec. Under steady-state bearing heating conditions, the critical speed for the disc with four-1 inch slots increased from 55.3 rev/sec to 60 rev/sec—both as measured and computed.

The disc resonant frequencies, which are on the ordinate at zero rotation in Fig. 4, are not constants. Accordingly, the critical speed is shifting continuously during operation, and at times variations due to thermal effects can be very large. The rotation speed for satisfactory operation is probably always below the critical speed at any time, and therefore conditions that tend to shift the critical speed down towards the operating rotation speed are destabilizing effects. The principal culprit is increased peripheral heating. When the critical speed approaches the operating speed, instability results. Conditions that tend to shift the critical speed upwards away from the operating speed are stabilizing influences—e.g., tensioning (Mote and Nieh 1971), bearing heating, or increased saw blade thickness. The critical speed concept provides a fundamental criterion for assessing the influence of combinations of process variations on the saw stability, emphasizes the need for a numerical facility to incorporate the significant process variables, and is useful as a basis for optimal saw design and on-line process control.

DATA ACQUISITION

The technique used to obtain the disc frequency spectrum experimentally (as in Figs. 1 and 2) is a hybrid experimental-numerical method (Nieh and Mote 1972). First, a few seconds of transverse displacement data are measured with a noncontacting, eddy-current-type transducer. The transducer has a linear range of ± 0.035 inch, a sensitivity of 10 mils/volt, and a frequency range 0–4 kHz. The deflection signal was filtered through a 4–840 Hz window with an attenuation of 30 db/octave. The data was then recorded on an FM instrumentation recorder at 30 inches/sec with signal/noise ratio of 44 db and a frequency range 0–5 kHz (± 0.5 db). The analog displacement data was then converted to 12 bit digital words at a rate of 2000 words/sec and stored on CDC compatible tapes. All data reduction operations were performed on the digitized form.

The spectral analysis of the digitized data is best computed using the Fast Fourier Transform algorithm of Cooley and Tukey (1965) in which the Fourier coefficients are smoothed with a digital filter. In the analysis 2048 data points or words were used, which gives a frequency band width of 0–1024 Hz at approximately 1 Hz intervals and requires 6.2 seconds of CDC 6400 computation time. The data points in Fig. 1 illustrate the results of such measurements and computations.

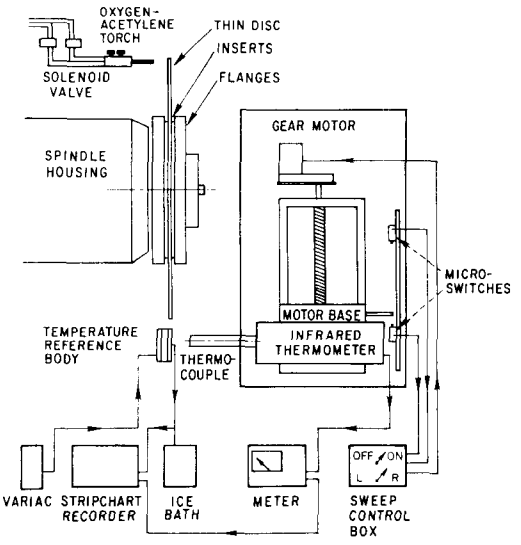

FIG. 5. Disc test stand with temperature measurement apparatus.

The external heat flux supplied to the disc was generated both by the spindle bearings and by an oxygen-acetylene torch (Fig. 5). The radiation sensor records the temperature in the range of 70–400 F, with an accuracy of ± 1% F.S., on a spot diameter of 0.15 inches, and with a response time of 2 seconds. With a thin spray of carbon black pigmented paint (emissivity 0.95–0.98) applied to the surfaces of the disc and reference body, the radial position accuracy obtained from the radiation sensor was ± 0.05 inches. The sensor was driven radially with a gear motor at a constant 0.035 in/sec rate. The time constant for the instrument is longer than is desirable, but at the time of its purchase other alternatives were not available. In order to modulate the time constant error, measurements were made both radially outward and inward, and the average can be used in the analysis. This technique can only be applied for steady-state measurements, and the error associated with the measurement technique is estimated to be ± 1 F.

HEAT TRANSFER

Heat transfer analysis is performed for investigation of the thermal problem itself, and for incorporation of thermal effects into the stability analysis. The modified conduction equation governing the steady-state temperature distribution is:

$$\frac{d\theta}{dr'^2} + \frac{1}{r'}\frac{d\theta}{dr'} - h_1\theta + \frac{\dot{q}b^2}{K_s} = 0 \qquad (1)$$

where

$h_1 = 2hb^2/K_s t$: modified Biot Number for two disc surfaces

K_s = disc thermal conductivity

$r' = r/b$

b = peripheral radius

t = disc thickness

θ = relative temperature

$\dot{q}$ = heat flux

h = convective heat transfer coefficient

This equation has been studied extensively (Sugihara and Sumiya 1955; Mote 1967), where for h_1 = constant exact θ solutions are determined for many cases. In saws, however, thickness is not usually constant and h_1 is not constant. The factor h is a function of air velocity across the surface and accordingly varies radially. It can be replaced by a weighted average value that would permit the elementary solution of (1), but this procedure needs further evaluation in the light of stability sensitivity to temperature variations. The convective coefficient in the laminar region is:

$$h_{lam} = C_1 K_a \left(\frac{\omega}{\nu}\right)^{0.5} = \text{constant} \qquad (2)$$

where K_a = air thermal conductivity, ω = disc angular velocity, ν = air kinematic viscosity, $C_1 = 0.35$ (Kreith 1958). In the turbulent region,

$$h_{turb} = C_2 K_a b^{0.6} \left(\frac{\omega}{\nu}\right)^{0.8} r'^{0.6} \qquad (3)$$

where coefficient values are either C_2 = 0.0185 (McComas and Hartnett 1970) or $C_2 = 0.0193$, (Cobb and Saunders 1956),

and the laminar to turbulent transition radius is

$$r'_{transition} = \left(\frac{250{,}000\nu}{\omega b^2}\right)^{0.5} . \quad (4)$$

Therefore, usually $h_1 = h_1(r')$ and (1) must be evaluated numerically. Finite element or finite difference representations of (1) are satisfactory and no difficulty is experienced because of discretization.

The external heat flux $\dot{q}$, which here arises from the spindle bearings and the peripheral torch, is generally unknown and is difficult to measure. The temperature distribution is measured, however, and an inverse iterative procedure can be used to estimate the $\dot{q}$ that would produce that temperature; here that heat flux is written $\hat{\dot{q}}$ to indicate its origin. At the present time there is no way to isolate the thermal analysis from experimental measurement, but temperature is more easily and accurately measured than heat flux so it is a logical choice. Therefore, we measure temperature and predict $\hat{\dot{q}}$.

In the first set of experiments the disc was rotated at constant angular velocity, and the heat flux was generated by the spindle bearings only. Measurement of the temperature distribution and the disc response for spectral analysis were recorded. Figure 6 shows a typical radial temperature distribution history for this type of heating. The temperature of the disc continued to

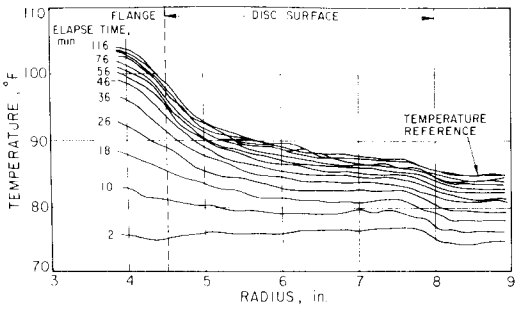

FIG. 6. Temperature distribution history of a uniform disc with bearing heating starting from room temperature. $\omega = 60$ rev/sec, $b = 8.0$ inches, $a = 4.0$ inches, $t = 0.040$ inches.

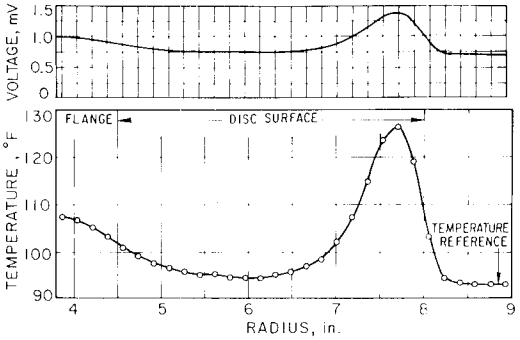

FIG. 7. Temperature data record and reduced temperature distribution of a disc with bearing and peripheral heating. Symbols are data points at 0.174 inch intervals. Disc contains four—1" long peripheral, radial slots. $\omega = 60$ rev/sec, $b = 8.0$ inches, $a = 4.0$ inches, $t = 0.040$ inch.

increase for approximately 2 hr, although the relative temperature reached a quasi-steady state after approximately 1 hr. Because the surrounding air temperature is not constant, it must be recorded. Radial air temperature variations were ignored; continuous data curves were sampled at 0.174-inch intervals (Fig. 7) and the curves were digitally plotted using a parabolic curve-fitting technique.

A number of important observations can be made from Fig. 6. First, there appears to be no such thing as a rotating disc at constant ambient temperature under conditions of rotation unless this temperature is externally maintained. Second, there is a long thermal transient period, but the principal variation occurs during the first half hour. Thirdly, the temperature variation under bearing heating alone is sufficient to increase the critical speed by 12% (Mote and Nieh 1971). Saw dynamic response is observed to be very sensitive to thermal effects, and crude approximations to the temperature distribution and level are probably unsatisfactory. As a direct practical observation, if saws are allowed to warm up (or even heated near the arbor) prior to use the probability of stable operation should be considerably higher.

Theory and experiment are compared in Fig. 8, in which C_2 is the coefficient of Eq. (3). In this case the published film coeffi-

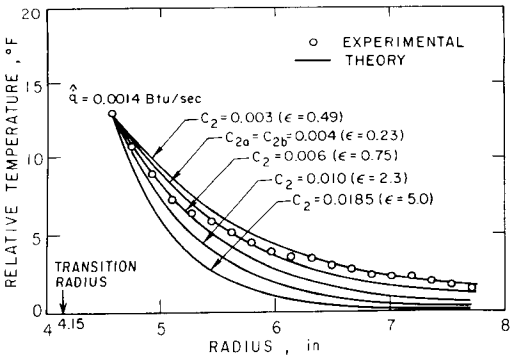

FIG. 8. Temperature distribution of a uniform disc with bearing heating. $\omega = 60$ rev/sec, b = 8.0 inches, a = 4.0 inches, t = 0.040 inch, C_{2a} = best coefficient for all bearing heating cases examined, C_{2b} = best coefficient for this bearing heating case, ϵ = mean square temperature error.

cient values $C_2 = 0.0185$ (McComas and Hartnett 1970) or $C_2 = 0.0193$ (Cobb and Saunders 1956) are seen to be too large and inapplicable. The probable explanation for this deviation is that the published coefficients were obtained from experiments with flat disc specimens. Air away from the disc moves toward the disc parallel to the axis of rotation, and upon reaching the disc the air flows along a curved path parallel to the disc plane. In the present case, the massive clamping collars disturb the convective air flow in the neighborhood of

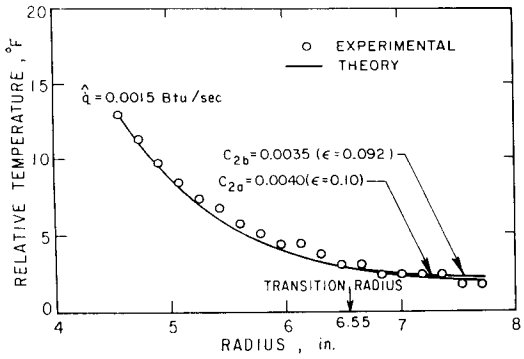

FIG. 9. Temperature distribution of a uniform disc with bearing heating. $\omega = 24$ rev/sec, b = 8.0 inches, a = 4.0 inches, t = 0.040 inch, C_{2a} = best coefficient for all bearing heating cases examined, C_{2b} = best coefficient for this bearing heating case, ϵ = mean square temperature error.

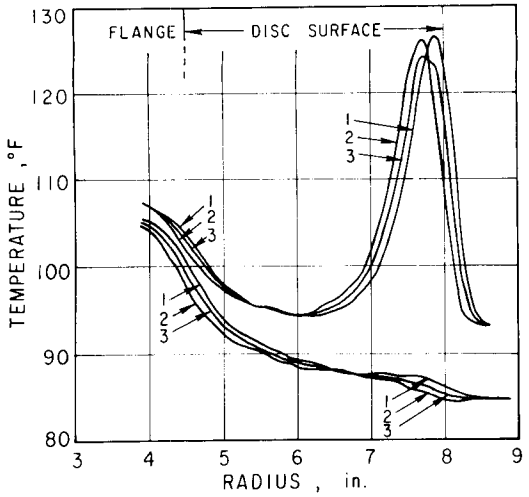

FIG. 10. Temperature distributions of a disc with bearing heating only and bearing plus peripheral heating. Disc contains four—1″ long, peripheral, radial slots. $\omega = 60$ rev/sec, b = 8.0 inches, a = 4.0 inches, t = 0.040 inch, 1—sensor sweep left to right, 2—sensor sweep right to left, 3—average.

the collars where the temperature is maximum. Because the convective air flow is inhibited from reaching the disc surface, one expects the convective heat transfer to be lower than that for an unclamped disc. Experiments conducted at 60 rev/sec, 40 rev/sec, and 24 rev/sec all exhibit the same effect (Fig. 9). The coefficient $C_2 = 0.004$ was found to give satisfactory results in the cases examined.

In a second set of thermal experiments, the torch was used to heat the disc periphery. Figure 10 gives a comparison of the quasi-steady state temperature distributions for the two experiment sets. The unfortunate instrument lag is clearly illustrated in this figure. This problem can be avoided with present commercially available instrumentation, but it did not seriously impair the conduct of our program. The principal uncertainty arises near the maximum temperature, which was not used here (Figs. 8 and 9). The distribution of heat flux near the periphery results from an inability to focus the torch on a spot. The heat from the bearings is seen to be a significant portion of the heat flux into the

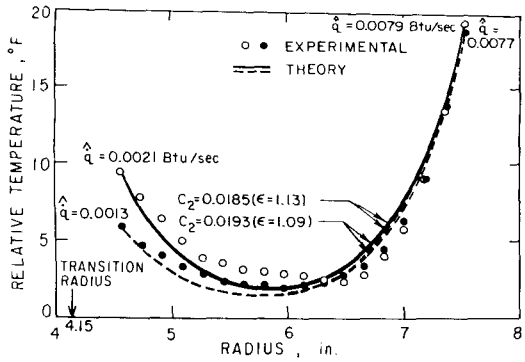

FIG. 11. Temperature distribution of a disc with bearing and peripheral heating. Solid points for uniform disc with mean square error $\epsilon = .40$. Open points for disc containing four—2″ radial, peripheral slots; mean square error ϵ as shown. $\omega = 60$ rev/sec, $b = 8.0$ inches, $a = 4.0$ inches, $t = 0.040$ inch.

disc. Note also that this thermal problem differs from that of the preceding paragraph in two ways. First, the high temperature region is away from the clamps where the published film coefficient research (Cobb and Saunders 1956; McComas and Hartnett 1970) can be expected to be more appropriate. Second, the convective action of the torch can only increase heat transfer and promote turbulence. The typical comparison of theory and experiment shown in Fig. 11 indicates that published C_2 values are very good here. Note that the theoretical prediction still underestimates the temperatures at small r (probably because of the clamping plates as before) and that it overestimates the temperature at large r because of the increased convective heat transfer induced by the torch and, in one case, the edge slots. The optimal heat transfer coefficient in turbulent flow is determined by Eq. (3) with $C_2 = 0.0193$ as suggested by Cobb and Saunders (1956). In a recent independent study Okushima and Sugihara (1969) experimentally determined C_2 to be 0.0194.

CONCLUSIONS

(i) Buckling and critical speeds are important and are the expected instability mechanism for *symmetrical* circular saws. Many saw-stability observations resulting from tensioning, thermal effects, etc., can be explained in terms of these concepts.

(ii) The influence of geometrical discontinuities, such as slots, on critical speed or buckling can be computed accurately. Their presence in the saw may or may not be beneficial to stability, depending upon the operating environment.

(iii) Critical speeds can be accurately computed by finite element methods if the temperature distribution is accurately known.

(iv) The temperature distribution may or may not be beneficial to stability, but its influence may be computed. Broadly speaking, a hot arbor is good for stability and a hot rim is bad for stability.

REFERENCES

COBB, E. C., AND O. A. SAUNDERS. 1956. Heat transfer from a rotating disk. Proc. Roy. Soc. (Ser. A):343–351.

COOLEY, J. S., AND J. W. TUKEY. 1965. An algorithm for the machine calculation of complex Fourier series, J. Math. Comput. 19: 297–301.

DUGDALE, D. S. 1966. Stiffness of a spinning disc clamped at its centre. J. Mech. Phys. Solids, 14:349–356.

KREITH, F. 1958. Principles of heat transfer. International Textbook Company, Scranton, Pa., pp. 326–327.

MCCOMAS, S. T., AND J. P. HARTNETT. 1970. Temperature profiles and heat transfer associated with a single disk rotating in still air. Fourth Int. Heat Transfer Conference, Heat Transfer 1970, Vol. 3.

MOTE, C. D., JR. 1967. Transient thermal stress and associated natural frequency variations in circular disk elements. Trans. ASME, 89(B):265–270.

MOTE, C. D., JR. 1970a. Formulation of discrete element models for stress and vibration analysis of plates. For. Prod. Lab. Rep. No. 35. 01.77, University of California.

MOTE, C. D., JR. 1970b. Unsymmetrical, transient heat conduction: rotating disk applications. Trans. ASME, 92(B):181–190.

MOTE, C. D., JR. 1971. Circular saw stability-fundamental considerations and specific research results. Proc. Wood Machining Seminar, University of California For. Prod. Lab., Richmond, March 24–25, pp. 15–38.

MOTE, C. D., JR. 1972. Stability control analysis of rotating plates by finite element: emphasis on slots and holes. J. Dyn. Syst. Meas. Control, Trans. ASME, 94(G), (1): 64–70.

MOTE, C. D., JR., AND L. T. NIEH. 1971. Control of circular disk stability with membrane stresses. Exp. Mech. 11(11):490–498.

NIEH, L. T., AND C. D. MOTE, JR. 1972. Rotating disc stability-spectral analysis and thermal effects. For. Prod. Lab. Res. Rep. University of California.

OKUSHIMA, S., AND H. SUGIHARA. 1969. Temperature distribution of circular saw blade-measurement with infrared radiometric microscope. J. Jap. Wood Res. Soc. 15(1):11–19.

SUGIHARA, H., AND K. SUMIYA. 1955. A theoretical study on temperature distribution of circular saw blade. Wood Res. Rev. 15:60–74.